JACS
JOURNAL OF THE AMERICAN CHEMICAL SOCIETY

Article

pubs.acs.org/JACS

Lipid Bilayer Crossing—The Gate of Symmetry. Water-Soluble Phenylproline-Based Blood-Brain Barrier Shuttles

Pol Arranz-Gibert,[†] Bernat Guixer,[†] Morteza Malakoutikhah,[†,‡] Markus Muttenthaler,[†] Fanny Guzmán,[§] Meritxell Teixidó,*[,†] and Ernest Giralt*[,†,∥]

[†]Institute for Research in Biomedicine (IRB Barcelona), Baldiri Reixac 10, Barcelona E-08028, Spain

[‡]Department of Chemistry, University of Isfahan, Isfahan 81746-73441, Iran

[§]Núcleo de Biotecnología Curauma, Pontificia Universidad Católica de Valparaíso, Valparaíso, Chile

[∥]Department of Organic Chemistry, University of Barcelona, Martí i Franquès 1-11, Barcelona E-08028, Spain

Supporting Information

ABSTRACT: Drug delivery to the brain can be achieved by various means, including blood-brain barrier (BBB) disruption, neurosurgical-based approaches, and molecular design. Recently, passive diffusion BBB shuttles have been developed to transport low-molecular-weight drug candidates to the brain which would not be able to cross unaided. The low water solubility of these BBB shuttles has, however, prevented them from becoming a mainstream tool to deliver cargos across membranes. Here, we describe the design, synthesis, physicochemical characterization, and BBB-transport properties of phenylproline tetrapeptides, $(PhPro)_4$, an improved class of BBB shuttles that operates via passive diffusion. These PhPro-based BBB shuttles showed 3 orders of magnitude improvement in water solubility compared to the gold-standard $(N\text{-MePhe})_4$, while retaining very high transport values. Transport capacity was confirmed when two therapeutically relevant cargos, nipecotic acid and L-3,4-dihydroxyphenylalanine (i.e., L-DOPA), were attached to the shuttle. Additionally, we used the unique chiral and conformationally restricted character of the $(PhPro)_4$ shuttle to probe its chiral interactions with the lipid bilayer of the BBB. We studied the transport properties of 16 $(PhPro)_4$ stereoisomers using the parallel artificial membrane permeability assay and looked at differences in secondary structure. Most stereoisomers displayed excellent transport values, yet this study also revealed pairs of enantiomers with high enantiomeric discrimination and different secondary structure, where one enantiomer maintained its high transport values while the other had significantly lower values, thereby confirming that stereochemistry plays a significant role in passive diffusion. This could open the door to the design of chiral and membrane-specific shuttles with potential applications in cell labeling and oncology.

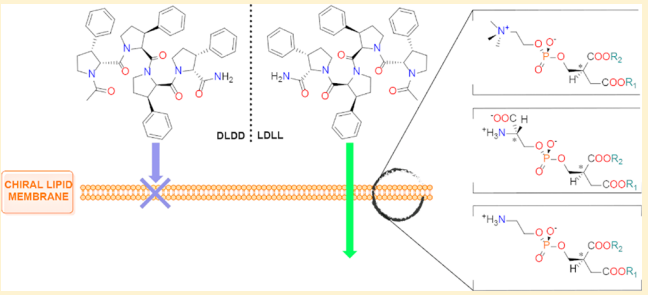

INTRODUCTION

Since the discovery of the blood-brain barrier (BBB) more than a century ago, considerable research effort has been devoted to this highly specialized cellular structure.[1] The BBB serves to protect our central nervous system (CNS) against external aggressions by regulating molecular transport through it.[2,3] Paracellular traffic at the endothelium of the BBB capillaries is constrained, since specialized structures, named tight junctions, prevent permeation through the intercellular cleft. Thus, molecular transport occurs mainly through a range of transcellular pathways (Figure 1).[4]

While the function of the BBB is essential, it also prevents therapeutics from reaching targets in the brain (>98% of low-molecular-weight drugs and almost 100% of large therapeutics do not cross the BBB).[2,5] For this reason, treatment of CNS diseases is seriously hindered, despite the high prevalence and socio-economic impact of these conditions.[5−7]

Diverse approaches have been pursued to overcome the BBB, ranging from invasive physical methods (i.e., neurosurgical-based approaches) to the use of chemically designed molecules capable of entering the brain (e.g., molecular Trojan horses).[5] The latter and more elegant means of delivering therapeutics into this organ requires applying our knowledge of the physiology, metabolism, and cellular structure of the BBB to rationalize the molecular design of drugs.

Several molecular pathways offer the key to the basal side of brain capillaries, the interior of the brain. Two major routes can be outlined, namely active and passive transport (Figure 1). Active transport implies carrier-mediated transport and endocytic mechanisms (receptor-mediated and adsorptive-mediated transcytosis)[4] that allow larger molecules like proteins or macromolecular complexes—and even viruses and bacteria—to cross the BBB.[8] The transport capacity is linked to cell dynamics, which is related to the number of receptors

Received: February 25, 2015
Published: May 20, 2015

DOI: 10.1021/jacs.5b02050
J. Am. Chem. Soc. 2015, 137, 7357−7364

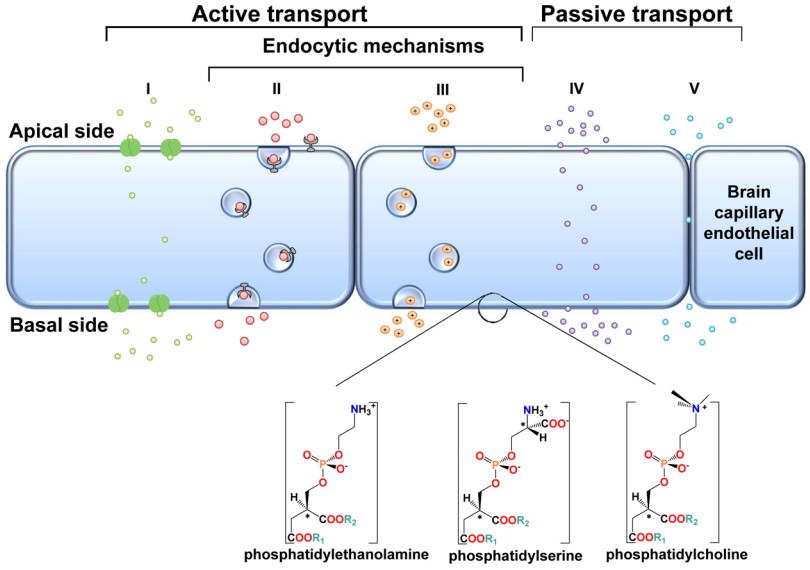

Figure 1. Transport mechanisms at the BBB. Active transport comprises (I) carrier-mediated transport and endocytic mechanisms ((II) receptor- and (III) adsorptive-mediated transcytosis), and passive transport comprises (IV) transcellular lipophilic diffusion and (V) paracellular hydrophilic diffusion. Transcellular lipophilic diffusion is dependent on the lipid composition of the cell, which comprises mainly phospholipids.

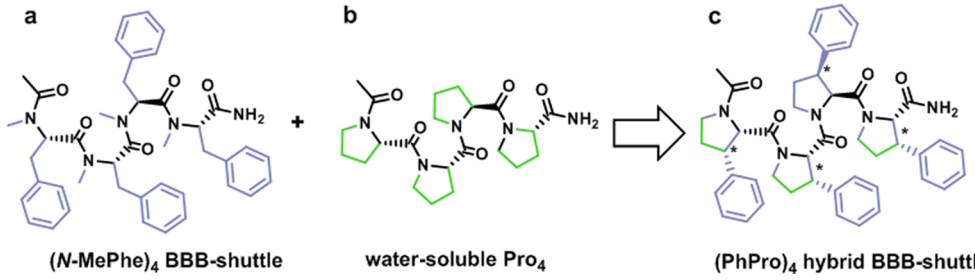

Figure 2. Structure of (a) the gold-standard passive diffusion BBB shuttle $(N\text{-MePhe})_4$, (b) hydrophilic polyproline unit Pro_4, and (c) designed $(PhPro)_4$ hybrid: all *homo*-L, *C*-terminal amide, and *N*-terminal acetylated.

present at the membrane,[9] thus leading to limited transport rates.[10]

Passive transport encompasses two main pathways, namely paracellular (hydrophilic) and transcellular (lipophilic) diffusion. The former allows small hydrophilic entities to cross the BBB. However, this pathway is extremely hindered at this barrier due to the presence of tight junctions,[4] and therefore it is not ideal for drug delivery. In contrast, transcellular lipophilic diffusion involves transport through the much larger lipid bilayer, which provides a direct correlation between concentration and transport. The lipid bilayer of the plasma membrane can be considered a *macroreceptor* that can interact simultaneously with many ligands, thus accounting for the greatest proportion of the cell surface. This layer is therefore the preferred target for the delivery of small-molecule therapeutic drugs.[2] Theoretically, transport through this mechanism is facilitated by the movement of the fatty acid side chains in the membrane, which form holes ("kinks") through which molecules can diffuse through the membrane.[11,12] The concentration of the kinks is estimated to be between 10 and 50 mM. This concentration is a function of the conformational changes that can be adopted by fatty acid hydrocarbon, which are related to the ratio of saturated/unsaturated fatty acids in the membrane and cholesterol.[13]

There are currently two main approaches to design therapeutics able to cross the BBB through transcellular lipophilic diffusion. The first, and most commonly implemented approach in the pharmaceutical industry, is based on a set of rules covering molecular size, presence of H-bond acceptors/donors, and lipophilicity, thereby attempting to increase the likelihood of the molecule crossing the BBB.[14,15] The second approach is the design of BBB shuttles, which forms a major research line in our laboratory.

BBB shuttles are molecular entities with the ability to carry cargos across the BBB through either active[16−18] or passive transport.[19] The great advantage of BBB shuttles is that they can confer the ability to cross the BBB to a wide range of molecules through simple conjugation chemistry. Thus, they are able to significantly expand the therapeutic space of potential CNS drugs, since compound selection is not limited to the otherwise highly restricted chemical space based on the above-mentioned rules. BBB shuttles can therefore act as powerful facilitators for drug delivery to the brain.

While chiral complexity in drug-receptor activation, receptor-mediated transcytosis, and protein−protein interactions has been studied extensively, the chiral interaction of entities with the membrane of the BBB endothelial cells is still poorly understood. Some studies have addressed a range of lipid structures,[20−22] and enantiomeric discrimination of dipeptides by biomembranes has also been reported.[23−25] However, the chiral interactions between the BBB and BBB shuttles have not been studied before. Considering the chiral nature of

DOI: 10.1021/jacs.5b02050
J. Am. Chem. Soc. 2015, 137, 7357−7364

phospholipids, one of the main components of plasma membranes, and our continuous efforts in improving BBB shuttle design, we set out to study the transport properties of different BBB shuttle stereoisomers. Additionally, we wanted to improve the water solubility of our BBB shuttles. Earlier work identified aromatic *N*-methylated peptides, both cyclic[19] and linear,[26−29] as highly permeable compounds for lipid membranes. Efforts in our laboratory led to the development of *N*-MePhe-based peptides, the gold-standard of passive diffusion BBB shuttles (Figure 2a).[27,28] The wider use of this class of BBB shuttles for clinical applications was, however, limited by the intrinsic low water solubility of these molecules (<1 μM).

Hence, we set out to advance the mechanistic knowledge and design opportunities of BBB shuttles by (i) studying the impact of chirality on their transport capabilities and (ii) improving their water solubility properties toward clinical applications. In order to achieve both goals, we sought to design and synthesize a library of novel chiral BBB shuttles that would provide further insight into the impact of chirality at the BBB, while at the same time tackling the long-standing problem of water solubility.

RESULTS

Peptide Shuttle Design. *N*-MePhe-based BBB shuttles[26−29] were taken as the base for the design of a new class of water-soluble BBB shuttles. Our aim was for these shuttles to retain high BBB effective permeability (P_e)[30] while improving their low water solubility. At the same time, we wanted to have control of chirality to study the transport capacity of different stereoisomers. For these purposes, we chose the proteogenic amino acid proline, which has a conformationally restricted side chain (advantageous for a chiral library design) and excellent water solubility (around 300 mM, the tetraproline), in spite of the hydrophobic character of its side chain. Additionally, polyprolines are also highly conformationally constrained compounds[31,32] that have been used extensively for the design of water-soluble dendrimers and cell-penetrating peptides (CPPs).[33]

We anticipated that a hybrid design of proline analogues containing a phenyl ring could merge the ability to cross the BBB with a simultaneous improvement of water solubility (Figure 2). Furthermore, phenyl and pyrrolidine rings have been described as two of the most common substructures in the chemical makeup of CNS drugs.[34] Thus, we turned our attention to peptides derived from *cis*-3-phenylpyrrolidine-2-carboxylic acid (PhPro, Figure 2c).

Transport Ability of $(PhPro)_4$ Shuttle Using the Parallel Artificial Membrane Permeability Assay (PAMPA). To establish whether this new hybrid class of BBB shuttles retained its anticipated transport properties, we used PAMPA to perform BBB transport studies of $(PhPro)_4$, which was initially synthesized with the commercially available racemic building block, Fmoc-*cis*-3-phenylpyrrolidine-2-carboxylic acid (Supporting Information (SI) Figure S1). The PAMPA assay, introduced by Kansy et al.,[35] allows the parallel evaluation of passive diffusion transport of various compounds through a mixture of lipids, thus emulating the biological barrier of interest. A selected lipid mixture is deposited onto a filter, which is divided into two compartments. Lipids are chosen as a function of the composition of the barrier; in our study, a mixture of porcine brain polar lipid extract was used. The compartments above and below the filter contained only buffer and the molecule to test in buffer, respectively. Magnetic stirring was applied for 4 h in donor wells, thus mimicking the stirring that red blood cells produce in brain capillaries. This approach almost totally reduced the unstirred water layer. Afterward, each well was quantified by UV absorption after injection into a RP-HPLC system. Time and concentration used were optimized to achieve a satisfactory signal-to-noise ratio during quantification and to prevent back-diffusion; i.e., the experiment was performed while the transport rate was constant. Finally, propranolol (a β-adrenergic receptor blocker with high brain penetration) was used as a positive control.

The formula for P_e calculation is shown in eq 1:

$$P_e = \frac{-218.3}{t}\log\left(1 - \frac{2C_A(t)}{C_D(t_0)}\right) \times 10^{-6} \text{ cm/s} \quad (1)$$

where t is the running time (4 h), $C_A(t)$ is the concentration of the compound in the acceptor well at time t, and $C_D(t_0)$ is the compound concentration in the donor well before running the PAMPA assay (t_0 = 0 h). Permeability is considered excellent with values >4.0 × 10^{-6}) cm/s, uncertain between 2.0 × 10^{-6} and 4.0 × 10^{-6} cm/s, and poor with values below 2.0 × 10^{-6}) cm/s.[30]

The suitability of the PhPro amino acid as a BBB shuttle building block was confirmed by comparing the transport of $(N\text{-MePhe})_4$, Pro_4, and $(PhPro)_4$ peptides, with *C*-terminal amide to confer higher stability and *N*-terminal acetylated to mimic the same charge state as when a cargo is attached (Table 1 and Figure 3a). The $(PhPro)_4$ tetrapeptide displayed transport properties similar to those of $(N\text{-MePhe})_4$. Pro_4, as expected,[28] displayed a marked reduction in transport, reaching almost zero (Table 1), highlighting the relevance of the phenyl ring—the most common molecular substructure in the chemical makeup of CNS drugs[34]—in the design of BBB shuttles.

Table 1. Transport and Effective Permeability (P_e) Values for *homo*-L Pro_4 and $(N\text{-MePhe})_4$ Peptides and the 16-Stereoisomer Mixture of $(PhPro)_4$ Peptide, as well as for $(N\text{-MePhe})_4$ and $(PhPro)_4$ Attached to a Therapeutically Relevant Cargo (L-DOPA or NIP) (n = 3; $x = \bar{x} \pm$ SD)[a]

compd	transport (%)	P_e (×10^6 cm/s)
Pro_4	0.02 ± 0.00	0.01 ± 0.00
$(N\text{-MePhe})_4$	12.7 ± 2.1	6.8 ± 1.3
$(PhPro)_4$	12.6 ± 0.3	6.88 ± 0.18
L-DOPA	0.0 ± 0.0	0.0 ± 0.0
L-DOPA-$(N\text{-MePhe})_4$	2.4 ± 0.2	1.10 ± 0.10
L-DOPA-$(PhPro)_4$	16.7 ± 1.7	9.9 ± 1.5
NIP	0.0 ± 0.0	0.0 ± 0.0
NIP-$(N\text{-MePhe})_4$	2.8 ± 0.2	1.40 ± 0.10
NIP-$(PhPro)_4$	19 ± 3	11 ± 2

[a]The transport values for *N*-MePhe-based peptides were published previously.[27,28]

Additionally, and in order to demonstrate the transport capacity of PhPro-based peptides as BBB shuttles, two therapeutically important cargos, nipecotic acid (NIP) and L-3,4-dihydroxyphenylalanine (L-DOPA), were coupled to the peptides (Figure 4) instead of an acetyl moiety.

L-DOPA is a prodrug that has been used for the past 40 years to treat Parkinson's disease.[36] It is transported to the CNS through large amino acid transporters[37] and enzymatically converted to dopamine by the aromatic L-amino acid

DOI: 10.1021/jacs.5b02050
J. Am. Chem. Soc. 2015, 137, 7357−7364

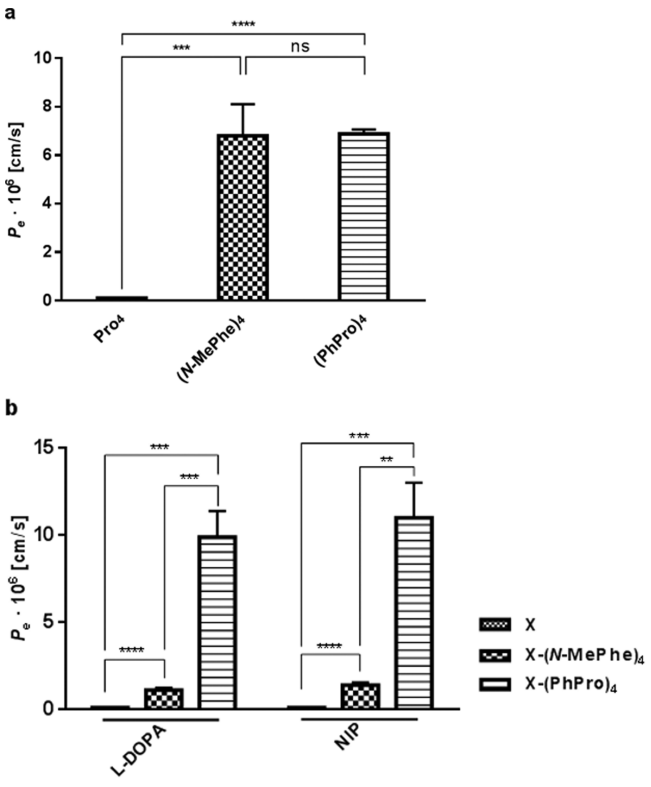

Figure 3. PAMPA transport values for (a) the initial peptides involved in the design of the water-soluble BBB shuttle: *homo*-L Pro_4 and $(N\text{-MePhe})_4$ peptides and the 16-stereoisomer mixture of $(PhPro)_4$ peptide. Additionally, the transport for (b) peptides attached to a cargo (L-DOPA and NIP) was evaluated, as well as that of the cargos alone ($n = 3$; $x = \bar{x} \pm SD$). Significance: ns ≡ not significant ($p \geq 0.05$), ** ≡ very significant ($0.001 \leq p < 0.01$), *** ≡ extremely significant ($0.0001 \leq p < 0.001$), **** ≡ extremely significant ($p < 0.0001$).

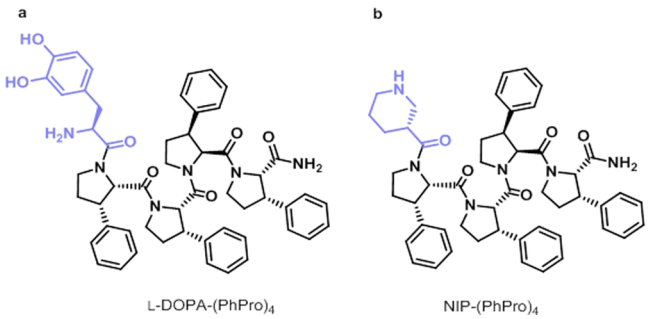

Figure 4. Structures for (a) L-DOPA-$(PhPro)_4$ and (b) NIP-$(PhPro)_4$ as *homo*-L configurations.

decarboxylase.[38,39] This conversion to dopamine occurs as well at the periphery, although it is limited when inhibitors of the aromatic L-amino acid decarboxylase are included in the therapy.[38] Nevertheless, other strategies based on L-DOPA derivatives are being developed to avoid side effects and focus the targeting at the CNS by means of increasing the delivery efficiency[40,41] or its selective conversion in there.[42]

NIP is a γ-aminobutyric acid (GABA) re-uptake inhibitor with great therapeutic potential if it could cross the BBB.[43−45] GABA is the primary inhibitory neurotransmitter in the CNS, and decreased levels of this molecule are associated with several brain disorders. The levels of this amino acid in the CNS can be increased either by supplying GABA or its agonists, or via GABA re-uptake inhibitors, such as NIP.

Hence, the BBB transport capacity of $(PhPro)_4$ peptide carrying L-DOPA or NIP was evaluated and compared to that of the gold-standard $(N\text{-MePhe})_4$ equivalent (Figure 3b). X-$(PhPro)_4$ was synthesized using Fmoc-SPPS (X = acetyl, L-DOPA, or NIP). PhPro-based peptides displayed permeability superior to that of their *N*-MePhe-based analogues. Unlike acetylated $(PhPro)_4$ peptide and its $(N\text{-MePhe})_4$ analogue, which did not display significant differences in permeability, $(PhPro)_4$ carrying either of the two cargos showed higher permeability (7-fold, with extremely significant differences) compared to its $(N\text{-MePhe})_4$ analogue. Furthermore, the ability to cross the BBB appeared to be independent of the type of cargo attached (i.e., its BBB shuttle capacity was not altered). This observation contrasted with the findings for the *N*-MePhe-based analogues, which showed a significant reduction in the capacity to cross the BBB (Table 1 and Figure 3). In contrast, the transport capacity of Pro_4 tetrapeptide was close to zero ($P_e = 0.01 \times 10^{-6}$ cm/s), as was that of the two cargos (NIP and L-DOPA).

Design and Synthesis of a 16-Stereoisomer Library of $(PhPro)_4$. In order to study the impact of chirality at the BBB, we devised a library of 16 stereoisomers of the $(PhPro)_4$ peptide (Figure 5). For the 16-stereoisomer library, we first had to separate the two PhPro enantiomers of the commercially available racemic mixture (SI Figure S2). After chiral separation of the two compounds, each PhPro enantiomer, L- and D-PhPro ((*S*,*S*)- and (*R*,*R*)-3-phenylpyrrolidine-2-carboxylic acid, respectively), was assigned by the specific rotation published previously.[46,47] All peptides were synthesized by manual Fmoc-SPPS.[48−50] The 16 stereoisomers of this library arose from the permutation of the two amino acid enantiomers in each position and were synthesized via Houghten's "tea bag" method.[51−53] All peptides were synthesized with a *C*-terminal amide to confer higher stability and were *N*-terminal acetylated to mimic the same charge state as when a cargo is attached.

Physicochemical Characterization of Pro_4 and $(PhPro)_4$ Shuttle. Circular dichroism (CD) studies were carried out to confirm the correct $(PhPro)_4$ enantiomeric assignment. The spectra of both *homo*-L and *homo*-D $(PhPro)_4$ were compared to those of the *homo*-L and *homo*-D Pro_4 analogue control peptides (synthesized with enantiomerically pure building blocks). As expected, the *homo*-L tetrapeptides (LLLL) displayed a negative CD spectrum, contrary to the *homo*-D (DDDD) ones, which displayed a positive one (SI Figure S4), thus confirming our initial assignment. The CD spectra of Pro_4 peptides recorded a higher signal, thereby suggesting a more defined secondary structure (i.e., PPII conformation generally observed with polyproline compounds[54] compared to the $(PhPro)_4$ tetrapeptides). The PhPro peptides studied by CD did not present a known structure-assigned spectrum.

Analytical RP-HPLC of the 16 stereoisomers further added to the characterization, showing complex chromatographic profiles (SI Figure S6) that were identical between pairs of enantiomers. Each peak of the profile corresponded to a conformer with an interconversion rate faster than (1/15) min^{-1} (length of the injection cycle), since re-injection of any of the collected peaks resulted in the same RP-HPLC chromatogram observed earlier (SI Figure S7a,c). In some cases, RP-HPLC characterization at higher temperature (60 °C) resulted in a single peak (SI Figure S7b). Only the

DOI: 10.1021/jacs.5b02050
J. Am. Chem. Soc. 2015, 137, 7357−7364

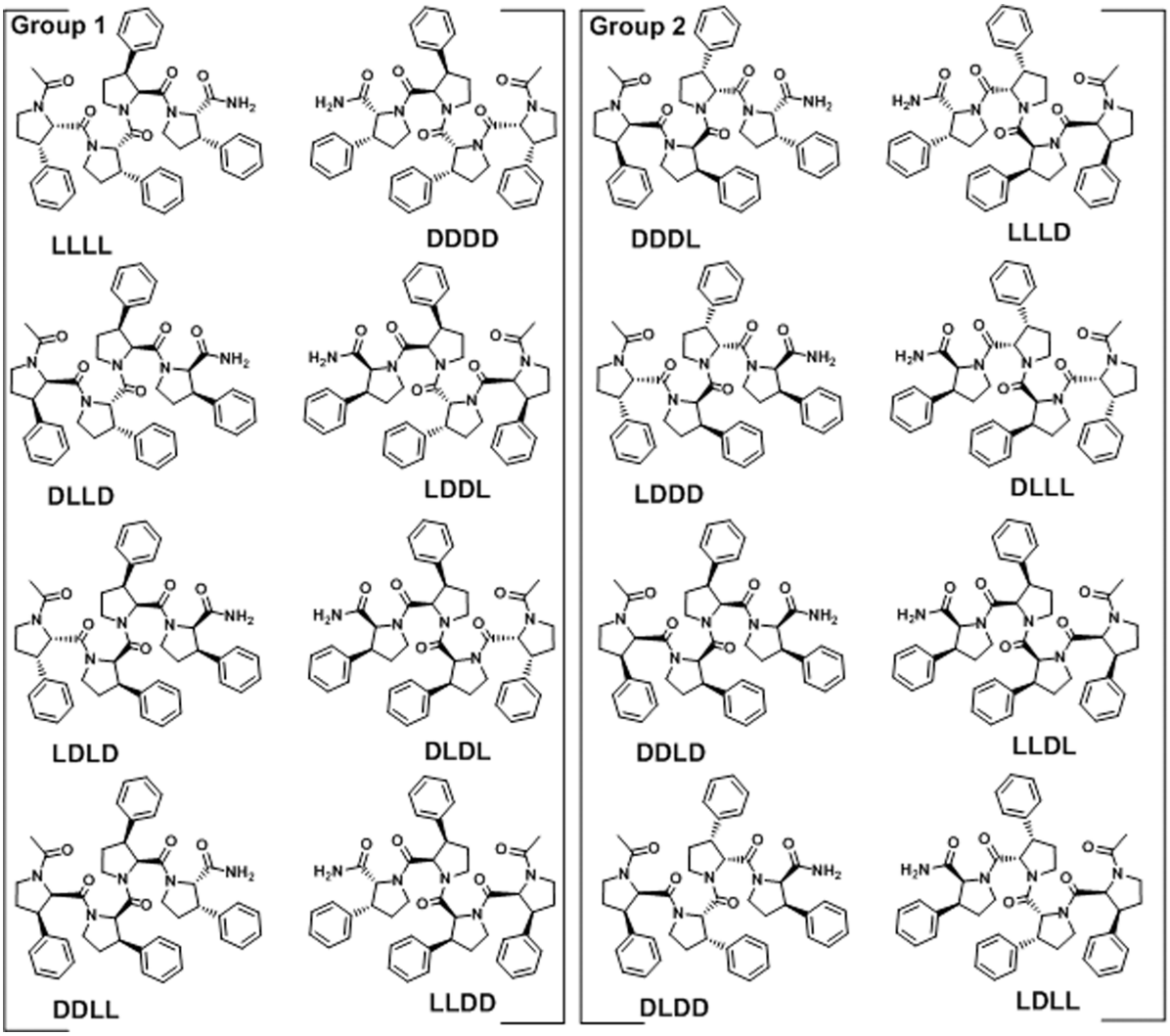

Figure 5. Library of the 16 $(PhPro)_4$ stereoisomers. The peptides are split into two transport-symmetry groups, where Group 1 contains the peptides with higher symmetry and lower enantiomeric discrimination, and Group 2 comprises the less symmetric peptides, related to a higher enantiomeric discrimination.

stereoisomers DDLD and LLDL yielded a single RP-HPLC peak, indicating a preferential conformational arrangement compared to the other stereoisomers. This observation was confirmed by CD, which showed a significantly different spectrum (maximum/minimum at 222 nm, respectively) compared to the other stereoisomers (SI Figure S5). Additionally, both of these enantiomers gelled after solvent (DIEA/DCM, 1:1, v/v) evaporation, thereby indicating the adoption of a specific conformational arrangement that favors this process (not observed with the other stereoisomers). Each peptide was identified by RP-HPLC-MS and MALDI-TOF MS, and the observed masses of the individual stereoisomers were in good agreement with the theoretically calculated molecular weights.

Water Solubility of $(PhPro)_4$ Shuttles. Since PhPro was chosen to improve the water solubility of these BBB shuttles, we determined this parameter by weighing the lyophilized peptide from a known volume of a saturated solution. The $(PhPro)_4$ tetrapeptides registered water solubility in the range of 1−5 mM, which can be considered a significant improvement (1000-fold) over that shown by $(N\text{-MePhe})_4$ tetrapeptides,[28] which dissolved only in the sub-micromolar range. The solubility of Pro_4 peptide was 300 mM. A relatively hydrophilic character was also observed when comparing the octanol/water partition coefficient, Log *P*, for the *homo*-L $(PhPro)_4$ (2.8) and *homo*-L $(N\text{-MePhe})_4$ (3.3). Equally, the 16-stereoisomer mixture of $(PhPro)_4$ displayed the same Log *P* as the *homo*-L $(PhPro)_4$. And finally, as expected, this parameter was −1.9 for *homo*-L Pro_4.

Passive Diffusion Transport Studies and Chiral Discrimination at the BBB. The passive diffusion of the 16-stereoisomer library of $(PhPro)_4$ through the BBB was evaluated using PAMPA (Figure 6).

Almost all the 16 stereoisomers displayed excellent transport properties (with P_e range of $(4.86–10) \times 10^{-6}$ cm/s), similar to the gold-standard $(N\text{-MePhe})_4$, which displays a transport capacity of 6.8×10^{-6} cm/s (Table 2 and Figure 6). Only DDLD and DLDD displayed significantly lower P_e values (3.64×10^{-6} and 0.85×10^{-6} cm/s, respectively). Interestingly, the DDLD/LLDL pair was identified earlier via analytical RP-HPLC and CD analysis, displaying a pronounced but distinct secondary structure compared to the other stereoisomers (SI Figure S5).

Chirality discrimination of the 16 stereoisomers at the BBB was determined by pairing the individual enantiomers and

DOI: 10.1021/jacs.5b02050
J. Am. Chem. Soc. 2015, 137, 7357−7364

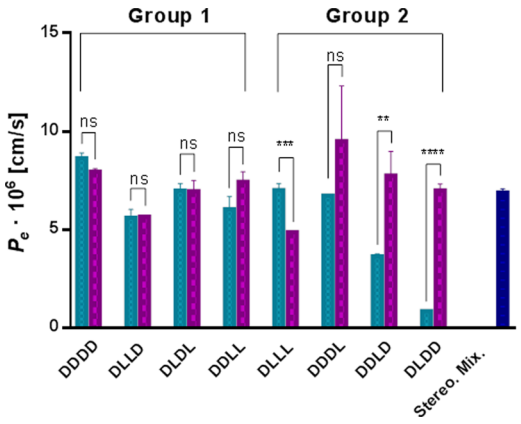

Figure 6. PAMPA transport values for the 16 individual stereoisomers, paired by enantiomers, and the 16-stereoisomer mixture (dark blue column). Light blue column corresponds to the peptide configuration displayed on the graph (e.g., first column = DDDD); purple column corresponds to the enantiomer of the peptide configuration displayed on the graph (e.g., first column = LLLL) (n = 3; $x = \bar{x} \pm$ SD). Significance: ns ≡ not significant ($p \geq 0.05$), ** ≡ very significant ($0.001 \leq p < 0.01$), *** ≡ extremely significant ($0.0001 \leq p < 0.001$), **** ≡ extremely significant ($p < 0.0001$).

Table 2. Transport and Effective Permeability (P_e) Values for the 16-Stereoisomer Library of $(PhPro)_4$ Peptide (n = 3; $x = \bar{x} \pm$ SD)

compd	transport (%)	P_e ($\times 10^6$ cm/s)
DDDD	15.2 ± 0.5	8.6 ± 0.3
LLLL	14.3 ± 0.3	7.95 ± 0.15
DDDL	12.34 ± 0.13	6.72 ± 0.07
LLLD	17 ± 5	10 ± 3
DDLD	7.1 ± 0.2	3.64 ± 0.13
LLDL	14 ± 2	7.8 ± 1.2
DLDD	1.76 ± 0.09	0.85 ± 0.04
LDLL	12.8 ± 0.6	7.0 ± 0.3
LDDD	9.27 ± 0.10	4.86 ± 0.05
DLLL	12.8 ± 0.6	7.0 ± 0.4
DDLL	11.2 ± 1.2	6.0 ± 0.6
LLDD	13.5 ± 0.9	7.4 ± 0.5
DLDL	12.7 ± 0.7	7.0 ± 0.4
LDLD	12.7 ± 1.0	7.0 ± 0.6
LDDL	10.61 ± 0.08	5.65 ± 0.04
DLLD	10.5 ± 0.8	5.6 ± 0.4
propranolol	22.6 ± 0.5	14.3 ± 0.3

determining the enantiomeric discrimination value (D_e) (Table 3). D_e is defined as the excess ratio of the transport of each pair of enantiomers, the higher (T_H) minus the lower (T_L), then divided by the lower (T_L):

$$D_e = \frac{T_H - T_L}{T_L} = \frac{T_H}{T_L} - 1 \quad (2)$$

By definition, this parameter ranges between 0 (no discrimination) and infinite (absolute discrimination). We observed values from 0.0 to 6.1 (Table 3). Differentially, the DLDD/LDLL pair of enantiomers showed the highest discrimination, followed by its *retro*-pair, DDLD/LLDL, which displayed a value of 1.0.

Table 3. Passive Diffusion Transport Enantiomeric Discrimination (D_e) Values for Each Pair of Enantiomers (n = 3; $x = \bar{x} \pm$ SD)[a]

group	enantiomer pair	enantiomeric discrimination
1	DLDL/LDLD	0.00 ± 0.00
	LDDL/DLLD	0.01 ± 0.08
	DDDD/LLLL	0.06 ± 0.04
	LLDD/DDLL	0.21 ± 0.13
2	DLLL/LDDD	0.38 ± 0.07
	LLLD/DDDL	0.4 ± 0.4
	LLDL/DDLD	1.0 ± 0.3
	LDLL/DLDD	6.1 ± 0.4

[a]Two groups are differentiated on the basis of the symmetry and enantiomeric discrimination: Group 1, higher symmetry, lower enantiomeric discrimination; Group 2, lower symmetry, higher enantiomeric discrimination.

DISCUSSION

Chirality plays a key role in many cellular processes, and we were interested if this is also the case during passive diffusion of BBB shuttles through the BBB. To study this phenomenon, we built a 16-stereoisomer tetrapeptide library via sequentially permuting each of the four positions with L- and D-PhPro enantiomers. The majority of the $(PhPro)_4$ stereoisomers displayed high diffusion through the BBB lipids, except for two peptides (DDLD and its *retro*-peptide DLDD), with significantly lower transport rates (Table 2 and Figure 6).

To further study the impact of chirality on the transport of this family of BBB shuttles, we classified pairs of enantiomers into two categories on the basis of the similarities in their transport (Table 2 and Figure 6). The peptide enantiomer pairs containing two units of each PhPro amino acid enantiomer in their sequence (DDLL/LLDD, DLDL/LDLD, and LDDL/DLLD) and the *homo*-peptides (LLLL/DDDD) showed similar transport between enantiomers (Group 1). Among this group, *homo*-peptides showed the highest transport and the LDDL/DLLD pair the lowest.

The transport values of the other enantiomer pairs with only one PhPro amino acid permutation (Group 2) varied significantly within the pairs (Figure 6). DDLD and its *retro*-peptide (DLDD) showed the poorest transport capacity (Table 2 and Figure 6), mainly due to membrane retention (60 and 87%, respectively; data not shown). Their enantiomers (LLDL and LDLL, respectively), however, showed excellent transport properties (7.8×10^{-6} and 7.0×10^{-6} cm/s, respectively), similar to those of Group 1. This clearly shows that, within two enantiomers, the transport properties can be significantly different (e.g., 7-fold for DLDD and LDLL), strongly suggesting that chirality plays an important role in passive diffusion.

In order to delve deeper into the chirality−transport relationship, a symmetry model was devised. Assuming two approximations, considering that the peptide termini (*N*-terminal acetylated and *C*-terminal amide) do not interfere in the symmetry and the peptide bond has no direction, i.e., *retro-enantiomeric* peptides would be identical,[55−57] two enantiomer pair groups were differentiated. Group 1, with the lowest enantiomeric discrimination (D_e) values, contains all *quasi-meso* isomers.[58] Group 2, with higher D_e values, lacks this *quasi-meso* character (and can be considered as less symmetric than Group 1). Furthermore, the pairs of enantiomers from Group 1 are

DOI: 10.1021/jacs.5b02050
J. Am. Chem. Soc. 2015, 137, 7357−7364

retro-enantio-peptides between them but not those belonging to Group 2. Interestingly, the LDLL/DLDD pair presented a very high D_e (6.1) (Table 3 and Figure 6).

In order to shed light on the structure of the $(PhPro)_4$ BBB shuttles, six peptides were studied by CD, namely the DDDD/LLLL pair (SI Figure S4b, red and blue, respectively), the DDLD/LLDL pair (SI Figure S5, red and blue, respectively), which presented differential properties (gel formation, single chromatographic peak, high enantiomeric discrimination), and *homo*-D and *homo*-L Pro_4 (SI Figure S4a, red and blue, respectively). While the CD spectra of the Pro_4 peptides showed a defined secondary structure (PPII), none of the $(PhPro)_4$ tetrapeptides presented a known structure-assigned spectrum. The spectrum of the DDLD/LLDL pair varied distinctively from the DDDD/LLLL pair, suggesting that its different secondary structure is the underlying reason for the observed physicochemical changes.

These results show that passive diffusion through biological membranes can be highly enantiomerically selective. Enantiomeric discrimination is a clear event in passive transport and can lead to high enantioselectivity. We could show that symmetry plays a crucial role in this process such that the greater the symmetry (Group 1), the lower the enantioselectivity. A desymmetrization step could therefore be employed to obtain compounds with high selectivity to distinct lipid compositions, i.e. different biological barriers, cell types, or disease regions, and even cellular regions, as the lipid composition differs among them.[59−67]

The second objective in this work was to analyze the water solubility of this new BBB shuttle class. Low water solubility represents a long-standing problem of current BBB shuttles with, for example, $(N\text{-MePhe})_4$, the gold-standard passive transport BBB shuttle, having a water solubility lower than 1 μM. The design choice of the $(PhPro)_4$ shuttle seemed to have the desired effect, improving water solubility by more than 3 orders of magnitude compared to $(N\text{-MePhe})_4$.

A preliminary study of the suitability of $(PhPro)_4$ to transport a therapeutically relevant cargo across the BBB was shown with L-DOPA and NIP. Although L-DOPA and NIP have enormous potential as CNS drugs,[68−70] neither one can cross the BBB by itself via passive diffusion (Table 1);[27,37] when they were attached to the PhPro-based shuttles, however, we observed excellent permeability. The transport of $(PhPro)_4$ carrying a cargo was around 7-fold higher compared to that of the *N*-MePhe shuttle (Table 1 and Figure 3). Furthermore, the transport capabilities of $(PhPro)_4$ are actually conferred to the cargo, in contrast to $(N\text{-MePhe})_4$, where a marked reduction can be observed once the shuttle is conjugated with the cargo (Table 1). Nevertheless, the pharmacokinetics and the pharmacodynamics of these conjugates remain unclear. In that way, several laboratories reported the use of L-DOPA prodrugs which can be administered either via parenterally[40] or orally,[71] including peptidyl derivatives,[41,71] glycoconjugates,[72] and glutathione peptidomimetics,[42] which all cross the BBB through carrier-mediated transport. Then, a modified version of our conjugates, containing a small linker selectively cleaved in the brain[42] and located in between the BBB shuttle and the cargo, could selectively release the drug in the CNS. Finally, the use of non-natural amino acids (and in some cases also the use of the D-amino acid version) has been shown in the literature to increase the resistance to proteolytic cleavage.[73−75] Thus, although not reported in this paper, one could speculate about the possibility of oral administration of these new PhPro-based conjugates.

CONCLUSIONS

Here we designed a new family of passive diffusion BBB shuttles based on the PhPro amino acid with superior water solubility and transfer capabilities compared to those of the $(N\text{-MePhe})_4$ gold-standard. Thus, overcoming the long-standing hurdle of low water solubility of passive diffusion BBB shuttles, PhPro-based shuttles have the potential to become very useful for brain delivery of drug candidates that are not able to cross the BBB unaided. Additionally, the transport study of the 16-stereoisomer library of $(PhPro)_4$ probed the impact of chirality on transport capability. This study showed that most stereoisomers maintained excellent transport capabilities, at the same time revealing two stereoisomers with significantly lower passive diffusion transport. This confirms that stereochemistry also plays a significant role in passive diffusion. We envisage in future work the intriguing possibility to design chiral shuttles with the unique potential to target membrane-specific cell types. This has potential applications in oncology, where it can be used to target tumors, since their membrane composition often differs significantly from that of healthy cells.[76−79]

ASSOCIATED CONTENT

Supporting Information

Materials, instrumentation, and experimental details, as well as complementary experimental data. The Supporting Information is available free of charge on the ACS Publications website at DOI: 10.1021/jacs.5b02050.

AUTHOR INFORMATION

Corresponding Authors

*meritxell.teixido@irbbarcelona.org
*ernest.giralt@irbbarcelona.org

Notes

The authors declare no competing financial interest.

ACKNOWLEDGMENTS

This work was supported by MINECO-FEDER (Bio2013-40716-R and RTC-2014-1645-1) and the *Generalitat de Catalunya* (XRB and 2014-SGR-521).

REFERENCES

(1) Rubin, L. L.; Staddon, J. M. *Annu. Rev. Neurosci.* **1999**, *22*, 11−28.
(2) Pardridge, W. M. *Drug Discovery Today* **2007**, *12*, 54−61.
(3) de Boer, A. G.; Gaillard, P. J. *Annu. Rev. Pharmacol. Toxicol.* **2007**, *47*, 323−355.
(4) Abbott, N. J. *J. Inherit. Metab. Dis.* **2013**, *36*, 437−449.
(5) Pardridge, W. M. *NeuroRX* **2005**, *2*, 3−14.
(6) Pringsheim, T.; Jette, N.; Frolkis, A.; Steeves, T. D. L. *Mov. Disord.* **2014**, *29*, 1583−1590.
(7) Hebert, L. E.; Weuve, J.; Scherr, P. A.; Evans, D. A. *Neurology* **2013**, *80*, 1778−1783.
(8) Kristensson, K. *Nat. Rev. Neurosci.* **2011**, *12*, 345−357.
(9) Cornford, E. M.; Hyman, S. *NeuroRX* **2005**, *2*, 27−43.
(10) Bickel, U. *NeuroRX* **2005**, *2*, 15−26.
(11) Träuble, H. *J. Membr. Biol.* **1971**, *4*, 193−208.
(12) Lieb, W.; Stein, W. *J. Membr. Biol.* **1986**, *92*, 111−119.
(13) Pardridge, W. M. *J. Neurochem.* **1998**, *70*, 1781−1792.
(14) Lipinski, C. A.; Lombardo, F.; Dominy, B. W.; Feeney, P. J. *Adv. Drug Delivery Rev.* **2012**, *64* (Supplement), 4−17.

DOI: 10.1021/jacs.5b02050
J. Am. Chem. Soc. 2015, 137, 7357−7364

(15) Wager, T. T.; Hou, X.; Verhoest, P. R.; Villalobos, A. *ACS Chem. Neurosci.* **2010**, *1*, 435−449.
(16) Prades, R.; Guerrero, S.; Araya, E.; Molina, C.; Salas, E.; Zurita, E.; Selva, J.; Egea, G.; López-Iglesias, C.; Teixidó, M.; Kogan, M. J.; Giralt, E. *Biomaterials* **2012**, *33*, 7194−7205.
(17) Wei, X.; Zhan, C.; Chen, X.; Hou, J.; Xie, C.; Lu, W. *Mol. Pharmaceutics* **2014**, *11*, 3261−3268.
(18) Gao, H.; Zhang, S.; Cao, S.; Yang, Z.; Pang, Z.; Jiang, X. *Mol. Pharmaceutics* **2014**, *11*, 2755−2763.
(19) Teixidó, M.; Zurita, E.; Malakoutikhah, M.; Tarragó, T.; Giralt, E. *J. Am. Chem. Soc.* **2007**, *129*, 11802−11813.
(20) Spector, M. S.; Selinger, J. V.; Singh, A.; Rodriguez, J. M.; Price, R. R.; Schnur, J. M. *Langmuir* **1998**, *14*, 3493−3500.
(21) Selinger, J. V.; Schnur, J. M. *Phys. Rev. Lett.* **1993**, *71*, 4091−4094.
(22) Lalitha, S.; Sampath Kumar, A.; Stine, K. J.; Covey, D. F. *J. Supramol. Chem.* **2001**, *1*, 53−61.
(23) Cruciani, O.; Borocci, S.; Lamanna, R.; Mancini, G.; Segre, A. L. *Tetrahedron: Asymmetry* **2006**, *17*, 2731−2737.
(24) Bombelli, C.; Borocci, S.; Cruciani, O.; Mancini, G.; Monti, D.; Segre, A. L.; Sorrenti, A.; Venanzi, M. *Tetrahedron: Asymmetry* **2008**, *19*, 124−130.
(25) Bombelli, C.; Borocci, S.; Lupi, F.; Mancini, G.; Mannina, L.; Segre, A. L.; Viel, S. *J. Am. Chem. Soc.* **2004**, *126*, 13354−13362.
(26) Chikhale, E.; Ng, K.-Y.; Burton, P.; Borchardt, R. *Pharm. Res.* **1994**, *11*, 412−419.
(27) Malakoutikhah, M.; Teixidó, M.; Giralt, E. *J. Med. Chem.* **2008**, *51*, 4881−4889.
(28) Malakoutikhah, M.; Prades, R.; Teixidó, M.; Giralt, E. *J. Med. Chem.* **2010**, *53*, 2354−2363.
(29) Malakoutikhah, M.; Guixer, B.; Arranz-Gibert, P.; Teixido, M.; Giralt, E. *ChemMedChem* **2014**, *9*, 1594−601.
(30) Di, L.; Kerns, E. H.; Fan, K.; McConnell, O. J.; Carter, G. T. *Eur. J. Med. Chem.* **2003**, *38*, 223−232.
(31) Chiang, Y.-C.; Lin, Y.-J.; Horng, J.-C. *Protein Sci.* **2009**, *18*, 1967−1977.
(32) MacArthur, M. W.; Thornton, J. M. *J. Mol. Biol.* **1991**, *218*, 397−412.
(33) Pujals, S.; Giralt, E. *Adv. Drug Delivery Rev.* **2008**, *60*, 473−484.
(34) Ghose, A. K.; Herbertz, T.; Hudkins, R. L.; Dorsey, B. D.; Mallamo, J. P. *ACS Chem. Neurosci.* **2011**, *3*, 50−68.
(35) Kansy, M.; Senner, F.; Gubernator, K. *J. Med. Chem.* **1998**, *41*, 1007−1010.
(36) Tomlinson, C. L.; Stowe, R.; Patel, S.; Rick, C.; Gray, R.; Clarke, C. E. *Mov. Disord.* **2010**, *25*, 2649−2653.
(37) del Amo, E. M.; Urtti, A.; Yliperttula, M. *Eur. J. Pharm. Sci.* **2008**, *35*, 161−174.
(38) Di Stefano, A.; Sozio, P.; Cerasa, L. *Molecules* **2008**, *13*, 46−68.
(39) Lloyd, K.; Hornykiewicz, O. *Science* **1970**, *170*, 1212−1213.
(40) Li, Y.; Zhou, Y.; Qi, B.; Gong, T.; Sun, X.; Fu, Y.; Zhang, Z. *Mol. Pharmaceutics* **2014**, *11*, 3174−3185.
(41) Tamai, I.; Nakanishi, T.; Nakahara, H.; Sai, Y.; Ganapathy, V.; Leibach, F. H.; Tsuji, A. *J. Pharm. Sci.* **1998**, *87*, 1542−1546.
(42) More, S. S.; Vince, R. *J. Med. Chem.* **2008**, *51*, 4581−4588.
(43) Barrett-Jolley, R. *Br. J. Pharmacol.* **2001**, *133*, 673−678.
(44) Ali, F. E.; Bondinell, W. E.; Dandridge, P. A.; Frazee, J. S.; Garvey, E.; Girard, G. R.; Kaiser, C.; Ku, T. W.; Lafferty, J. J.; Moonsammy, G. I.; Oh, H. J.; Rush, J. A.; Setler, P. E.; Stringer, O. D.; Venslavsky, J. W.; Volpe, B. W.; Yunger, L. M.; Zirkle, C. L. *J. Med. Chem.* **1985**, *28*, 653−60.
(45) Krogsgaard-Larsen, P.; Johnston, G. A. R. *J. Neurochem.* **1975**, *25*, 797−802.
(46) Flamant-Robin, C.; Wang, Q.; Chiaroni, A.; Sasaki, N. A. *Tetrahedron* **2002**, *58*, 10475−10484.
(47) Belokon, Y. N.; Bulychev, A. G.; Pavlov, V. A.; Fedorova, E. B.; Tsyryapkin, V. A.; Bakhmutov, V. A.; Belikov, V. M. *J. Chem. Soc., Perkin Trans. 1* **1988**, 2075−2083.
(48) Merrifield, R. B. *J. Am. Chem. Soc.* **1963**, *85*, 2149−2154.
(49) Fields, G. B.; Noble, R. L. *Int. J. Pept. Protein Res.* **1990**, *35*, 161−214.
(50) Carpino, L. A.; El-Faham, A.; Minor, C. A.; Albericio, F. *J. Chem. Soc., Chem. Commun.* **1994**, 201−203.
(51) Houghten, R. A. *Proc. Natl. Acad. Sci. U.S.A.* **1985**, *82*, 5131−5135.
(52) Houghten, R. A.; Pinilla, C.; Blondelle, S. E.; Appel, J. R.; Dooley, C. T.; Cuervo, J. H. *Nature* **1991**, *354*, 84−86.
(53) Houghten, R. A. *Annu. Rev. Pharmacol. Toxicol.* **2000**, *40*, 273−282.
(54) Bochicchio, B.; Tamburro, A. M. *Chirality* **2002**, *14*, 782−792.
(55) Goodman, M.; Chorev, M. *Acc. Chem. Res.* **1979**, *12*, 1−7.
(56) Freidinger, R. M.; Veber, D. F. *J. Am. Chem. Soc.* **1979**, *101*, 6129−6131.
(57) Li, C.; Pazgier, M.; Li, J.; Li, C.; Liu, M.; Zou, G.; Li, Z.; Chen, J.; Tarasov, S. G.; Lu, W.-Y.; Lu, W. *J. Biol. Chem.* **2010**, *285*, 19572−19581.
(58) By *quasi-meso* we mean compounds that, assuming that the peptide termini are not relevant and the peptide bond does not have directionality, have an accessible achiral conformation and therefore would be *meso* forms.
(59) Spector, A. A.; Yorek, M. A. *J. Lipid Res.* **1985**, *26*, 1015−35.
(60) Lingwood, D.; Simons, K. *Science* **2010**, *327*, 46−50.
(61) Yechiel, E.; Barenholz, Y. *J. Biol. Chem.* **1985**, *260*, 9123−9131.
(62) Boesze-Battaglia, K.; Schimmel, R. *J. Exp. Biol.* **1997**, *200*, 2927−36.
(63) Edidin, M. *Annu. Rev. Biophys. Biomol. Struct.* **2003**, *32*, 257−283.
(64) Simons, K.; Ikonen, E. *Nature* **1997**, *387*, 569−572.
(65) Kummerow, F. A. *Ann. N.Y. Acad. Sci.* **1983**, *414*, 29−43.
(66) SoOderberg, M.; Edlund, C.; Alafuzoff, I.; Kristensson, K.; Dallner, G. *J. Neurochem.* **1992**, *59*, 1646−1653.
(67) Norton, W. T.; Abe, T.; Poduslo, S. E.; DeVries, G. H. *J. Neurosci. Res.* **1975**, *1*, 57−75.
(68) Katzenschlager, R.; Poewe, W. *Nat. Rev. Neurol.* **2014**, *10*, 128−129.
(69) Olanow, C. W.; Obeso, J. A.; Stocchi, F. *Lancet Neurol.* **2006**, *5*, 677−687.
(70) Vossler, D. G.; Morris, G. L., III; Harden, C. L.; Montouris, G.; Faught, E.; Kanner, A. M.; Fix, A.; French, J. A. *Epilepsy Behavior* **2013**, *28*, 211−216.
(71) Bai, J. F. *Pharm. Res.* **1995**, *12*, 1101−1104.
(72) Bonina, F.; Puglia, C.; Rimoli, M. G.; Melisi, D.; Boatto, G.; Nieddu, M.; Calignano, A.; Rana, G. L.; Caprariis, P. d. *J. Drug Targeting* **2003**, *11*, 25−36.
(73) Lien, S.; Lowman, H. B. *Trends Biotechnol.* **2003**, *21*, 556−562.
(74) Miller, S. M.; Simon, R. J.; Ng, S.; Zuckermann, R. N.; Kerr, J. M.; Moos, W. H. *Drug Dev. Res.* **1995**, *35*, 20−32.
(75) Prades, R.; Oller-Salvia, B.; Schwarzmaier, S. M.; Selva, J.; Moros, M.; Balbi, M.; Grazú, V.; de La Fuente, J. M.; Egea, G.; Plesnila, N.; Teixidó, M.; Giralt, E. *Angew. Chem.* **2015**, *127*, 4039−4044.
(76) Santos, C. R.; Schulze, A. *FEBS J.* **2012**, *279*, 2610−2623.
(77) Maxfield, F. R.; Tabas, I. *Nature* **2005**, *438*, 612−621.
(78) van Meer, G.; Voelker, D. R.; Feigenson, G. W. *Nat. Rev. Mol. Cell. Biol.* **2008**, *9*, 112−124.
(79) Li, Y. C.; Park, M. J.; Ye, S.-K.; Kim, C.-W.; Kim, Y.-N. *Am. J. Pathol.* **2006**, *168*, 1107−1118.

DOI: 10.1021/jacs.5b02050
J. Am. Chem. Soc. 2015, 137, 7357−7364